

# Research on Feature Extraction of Halftone Image

Zhiqiang Wen, Yongxiang Hu, Wenqiu Zhu

School of Computer & Communication Hunan University of Technology Hunan Zhuzhou, China

Email: zhqwen20001@163.com, huyx506@163.com, wenqiu\_zhu@126.com

**Abstract**—A new feature extraction method based on multi-directional correlation function is proposed for improving the classification performance of halftone images in this paper. The correlation function is improved to obtain feature vectors on three directions of halftone images. Based on the definition of pixel probability, pixel entropy and entropy histogram, we introduce a decision rule to reject some invalid halftone images. We describe the details about feature extraction algorithm of halftone image. The experiment results show the proposed method is effective.

**Index Terms**—halftone image, feature extraction, inverse halftoning, multi-directional correlation

## I. INTRODUCTION

Digital halftoning is the process of converting continuous tone images into images with a limited gray levels to create the perception of a continuous tone image via using the limited gray level discrimination capability and the low-pass characteristics of the spatial sensitivity of the human visual system. Inverse halftoning, which belongs to image restoration, is the inverse process of digital halftoning and has been widely used in paper image digitization, digital publishing system and image processing. Most of the recent researches focus on the inverse halftoning based on a kind of halftone image. Stochastic model [1] and the maximizer of posterior marginal estimation [2] were presented respectively to restore a continuous-tone image of ordered dither image. The inverse halftoning based on markov random field and maximum a posteriori[3] and the space-scale domain projection [4] were provided respectively to reconstruct a continuous tone image from an error diffusion image. M. Mese, et al used projection onto convex sets to reconstruct continuous tone image of dot diffusion image [5]. However, it is difficult to obtain the optimal reconstruction quality because of unknown halftoning type in these inverse halftoning algorithms in applications. To solve this problem, it is necessary to develop a classification mechanism, which can distinguish different various halftoning images before reconstructing continuous tone image.

Until now, only several classification methods of halftone images are presented. In 1997, P. C. Chung, et al first used the enhanced one-D correlation to extract the features of halftone images and utilized back-propagation (BP) neural network as the classification method [6]. Y. P.

Kong, et al employed the enhanced one-D correlation function and gray level co-occurrence matrix to extract the features of a halftone image and used decision tree to classify halftone images [7]. Y. F. Liu, et al extracted features from Fourier spectrum of nine type of halftone image by least mean square (LMS) algorithm and used naive Bayesian to classify halftone images [8].

In this paper we focus on feature extraction of halftone image to improve the classification correct rate and reduce the computation cost. We have three contributions: 1) we present a new feature extraction method based on multi-directional correlation. 2) We present a decision rule to reject the invalid halftone images and discuss a lot of details about this rule. 3) We present a wide range of experiments to evaluate the effectiveness of our methods and provide a comprehensive comparison.

The rest of this paper is organized as follows. We present a new feature extraction method in section 2 and the experiment results are presented in section 3. In section 4 we conclude this paper.

## II. FEATURE EXTRACTION METHOD

Among all kinds of halftoning algorithms, ordered dither, error diffusion and dot-diffusion are three kinds of most popular methods in printing industry at present. Due to depending on the screen matrix, each kind of these algorithms may include many branch algorithms, from which, twelve classical halftoning algorithms are carefully selected to generate halftone images for classification and more details are shown in TABLE I. Fig.1 shows the halftone images of “Lena” generated by above twelve kinds of classical halftoning algorithms. Different halftoning algorithms will lead to different image texture characteristic, so the texture extraction methods are employed in this paper.

The texture extraction methods can be divided into two categories: transform domain and spatial domain. The former extract the features from image transform domain, such as Fourier spectrum, to feed a classifier [8]. The disadvantages of using the former is that it need large amount of calculation. The latter will extract statistical invariant features of halftone image, such as correlation statistical characteristic [6] or gray level co-occurrence matrix [7], as the input of a classifier. This kind of method is simple and has good practical value. We choose the latter and focus on correlation feature extraction of halftone image.

TABLE I.  
HALFTONING ALGORITHMS AND THEIR DETAILS

No.	Abbr.	algorithms	Details about methods
1	Bayer	disperse dither	Bayer 8×8 matrix and 64 gray level [9]
2	Clu8	cluster dither	Cluster Dither 8×8 matrix and 64 gray level [9]
3	Clu4	cluster dither	Cluster Dither 4×4 matrix and 16 gray level [9]
4	Knu8	dot-diffusion	Knuth 8×8 matrix and 64 gray level [10]
5	Knu4	dot-diffusion	Knuth 4×4 matrix and 16 gray level [10]
6	Disp8	disperse dither	Dot local Cluster and entirety diffusion 8×8 matrix [9]
7	Stu	error diffusion	Stucki filter[11]
8	Jar	error diffusion	Jarvis filter [11]
9	Flo	error diffusion	Floyd-Steinberg filter [11]
10	Sten	error diffusion	Stenenson filter [11]
11	Mes8	dot-diffusion	Mese-Vaidyanathan 8×8 matrix [12]
12	Mes16	dot-diffusion	Mese-Vaidyanathan 16×16 matrix [12]



Figure 1. Twelve halftone images (“Lena”, 256\*256) where the number of sub-image is corresponds to the number in Table 1 from left to right and from top to bottom.

#### A. Multi-directional Correlation Feature

Let  $f$  denotes a continuous-tone image and  $f(x, y)$  denotes the pixel in image position  $(x, y)$  where  $0 \leq f(x, y) \leq 255$ . The general correlation function can be defined as follows.

$$C(\varepsilon, \eta, j, k) = \frac{\sum_{m=j-w}^{j+w} \sum_{n=k-w}^{k+w} f(m, n) f(m - \varepsilon, n - \eta)}{\sum_{m=j-w}^{j+w} \sum_{n=k-w}^{k+w} [f(m, n)]^2} \quad (1)$$

where  $\varepsilon, \eta = 0, \pm 1, \dots, \pm T$ . Expression (1) describes the correlation value between two pixels in window  $(2w+1) \times (2w+1)$ . Second order moment is regarded as the measurement of correlation function as

$$T(j, k) = \sum_{\varepsilon=-T}^j \sum_{\eta=-T}^j \varepsilon^2 \eta^2 C(\varepsilon, \eta, j, k) \quad (2)$$

But the computation cost of (2) is very large. A revised method, as shown in (3), is to use the enhanced one-D correlation (EODC) [6] to extract the texture features.

$$r(l) = \frac{1}{MN} \sum_{i=0}^{M-1} \sum_{j=0}^{N-1} H(a+i, b+j) \cdot H(a+i, b+j+l) \quad (3)$$

where  $H(a, b)$  denotes the sub-block of a halftone image and  $a, b = 0, 1, \dots, M-1$ .  $l = 1, 2, \dots, L$  and generally let  $L = 16$ . The sub-block size is set as  $1 \times L$  [6]. Compared to (2), the computation cost ( $O(MNL^2)$ ) of (3) drop a lot but is still large. To solve this problem, this paper presents a fast feature extraction of multi-direction correlation (MDC). In our method, the correlation between not two sub-blocks but two pixels in three directions is utilized to obtain feature vectors. Furthermore, XNOR operation in logic is used to compute correlation value between two pixels since the halftone image is a special case that there are only two values (0 and 1). More details are given as

1) 0 degree

$$r_1(l) = \sum_{i=0}^{M-1} \sum_{j=0}^{N-1} f(i, j) \circ f(i+l, j) \quad (4)$$

2) 45 degree

$$r_2(l) = \sum_{i=0}^{M-1} \sum_{j=0}^{N-1} f(i, j) \circ f(i+l, j+l) \quad (5)$$

3) 90 degree

$$r_3(l) = \sum_{i=0}^{M-1} \sum_{j=0}^{N-1} f(i, j) \circ f(i, j+l) \quad (6)$$

where sign “ $\circ$ ” denotes the XNOR operation and  $1 \leq l \leq L$  ( $L$  is a constant). We can obtain three vectors  $r_1, r_2$  and  $r_3$  via (4), (5) and (6) to form a new feature vector  $R$ , by  $R = [r_1 \ r_2 \ r_3]$ . The length of vector  $R$  is  $3L$ . After normalizing vector  $R$ , we can get  $3L$  correlation features of a halftone image. Since the computation cost of (4), (5) and (6) are  $O(MNL)$  respectively, the total computation cost is  $O(MNL)$ .

#### B. Decision Rule for Effective image

Smooth continuous-tone images will almost result in the same texture feature, for example, most of pixels in a halftone image are black (1) or white (0) as shown in Fig.2. These halftone images do not provide enough texture information for classifier, that is to say, these halftone images are inseparable. So we must ignore these halftone images before feature extraction. These inseparable images are named as invalid images and the other images are known as effective images. As a

consequence, we will use a general inverse halftone method for reconstruction of these inseparable images. The purpose of this section is to present a method of finding the effective images from all halftone images. For this purpose, we give the definition of pixel probability, pixel entropy and probability histogram of a halftone image, and then present a decision rule.

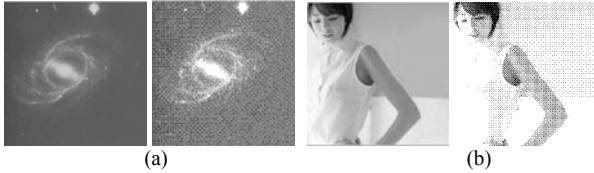


Figure 2. Two example of halftone image (Bayer) where left is original images and right is the halftone images in (a), (b)

**Definition 1.** Pixel probability of halftone image is defined as

$$p_i = n_b / (n_w + n_b)$$

where  $n_b$  ( $n_w$ ) is the number of black (white) pixels in neighborhood of  $i$ th pixel. The size of neighborhood is set as  $5 \times 5$  in experiments. Pixel probability  $p_i$  describes the distribution of the black pixel in neighborhood of the  $i$ th pixel. The larger of  $n_b$  value, the higher of  $p_i$ .  $p_i = 1$  (0) indicates that the neighborhood of  $i$ th pixel only contain the black (white) pixels, and  $p_i = 0.5$  shows that number of black pixels and white pixels in the neighborhood of  $i$ th pixel are equal.

**Definition 2.** Pixel entropy of a halftone image is defined as

$$H_i = \sum_{j \in \Phi(i)} \log(p_j) p_j$$

where  $p_j$  is the pixel probability of  $j$ th pixel in neighborhood  $\Phi$  of  $i$ th pixel. Pixel neighborhood size is  $9 \times 9$  in experiments. Pixel entropy  $H_i$  reflects the carried information of a halftone image. As proven by information theory, the maximum amount information is available when the numbers of black pixel and white pixel are equal. However, it is still not enough to fully describe the stableness and distribution of the information in a halftone image by only using pixel entropy. So we give the definition of entropy histogram of a halftone image.

**Definition 3.** Entropy histogram of a halftone image is defined as

$$h_u = C \sum_{i=1}^n \delta(b(H_i) - u)$$

where  $n$  is the pixel number of a halftone image, and  $u=1, \dots, m$  ( $m$  is the width of entropy histogram and  $m=20$  in experiments).  $\delta(\bullet)$  is a Kronecker delta function and  $b(\bullet)$  is a mapping function from pixel entropy to entropy histogram.  $b(\bullet)$  is set as:  $b:(H_i - H_{min})/s \rightarrow \{1, \dots, m\}$ , where  $s=(H_{max} - H_{min})/(m-1)$ ,  $H_{max} = \max\{H_i\}$ , and  $H_{min} = \min\{H_i\}$  ( $i=1, \dots, n$ ). Table 2 shows six entropy histograms which describe the distribution of black pixel in six halftone images. Most of pixels in No.1 and No.2 (No.3 and No.4) in TABLE II are black (white) pixels. In these examples, most of bin values in entropy histogram concentrate in low pixel entropy range, but in other cases such as No.5

and No.6 in TABLE II, most of bin values concentrate in high pixel entropy. Therefore, we calculate mean and variance of pixel entropy which can determine whether the halftone image is effective. Calculation method of mean and variance is as follows.

$$\mu = \frac{1}{n} \sum_{i=1}^n H_i \tag{7}$$

$$\sigma = \sqrt{\frac{1}{n} \sum_{i=1}^n (H_i - \mu)^2} \tag{8}$$

The greater  $\mu$  of entropy histogram is, the more uniform the distribution of black pixels is. The large  $\sigma$  of entropy histogram will lead to concentrated distribution of pixel entropy. Therefore, it requires large  $\mu$  and small  $\sigma$ . The decision rule is: if  $\mu > \mu_{\text{thresh}}$  and  $\sigma < \sigma_{\text{thresh}}$ , this halftone image is accepted as an effective image, otherwise it is rejected as an invalid image. In this rule,  $\mu_{\text{thresh}}$  and  $\sigma_{\text{thresh}}$  are two previously set threshold value.

TABLE II. EXAMPLES OF HALFTONE IMAGE AND ENTROPY HISTOGRAM (BAYER)

No.	continuous-tone image	halftone images	entropy histogram
1			
2			
3			
4			
5			
6			

C. Feature Extraction Algorithm

According to our ideas, a halftone image is divided into many sub-image blocks with the same size and each effective sub-image block is decided by above decision rule. Let  $B_i$  denotes the  $i$ th sub-image block with same size  $K \times K$  of a halftone image. Let  $\mathbf{R}_i$  denotes the feature vector of sub-image block  $B_i$  and  $\mathbf{T}$  is the feature vector of the halftone image, satisfying:  $|\mathbf{T}| = |\mathbf{r}| = 3L$ . Proposed feature extraction algorithm is as follows:

**Step 1:** Divide the halftone image  $f$  into sub-image block  $B_i$  ( $i=1, \dots, n$ ) with size  $K \times K$  and initialize  $\mathbf{T}$  to 0. Let  $i=1$ .

**Step 2:** Calculate  $\mu$  and  $\sigma$  of  $B_i$  via (7) and (8).

**Step 3:** Decide whether  $B_i$  is effective by above presented decision rule. If  $B_i$  is effective, turn to step 4, otherwise turn to step 6.

**Step 4:** Calculate  $r_1, r_2$  and  $r_3$  of  $B_i$  according to (4), (5) and (6).

**Step 5:** Let  $R=[r_1 r_2 r_3]$  and  $T=T+R_i$

**Step 6:** If  $i>n$ , turn to step 7, otherwise,  $i=i+1$  and turn to step 2.

**Step 7:** If  $T \neq 0$ , normalize  $T$ , otherwise, regard this image as an invalid image.

### III. EXPERIMENTAL RESULTS

We use VC++6.0 and Open CV as programming tool under the environment of Windows XP, and computer with Intel chip, 2.2GHz CPU frequency and 3G RAM. The image sets are from two public dataset (<http://decsai.ugr.es/cvg/dbimagenes/>) including 1 000 original continuous tone image ( $256 \times 256$ ). Each of the original image is transformed into twelve halftone images respectively by above twelve halftoning algorithms, therefore, there are 12 000 halftone images where 6 000 halftone images are regarded as the training samples and the others form the test samples.

#### A. Experiment 1

This experiment studies the behaviors of selection on effective halftone images with different threshold. A large number of samples are used to determine the parameter strategies of  $\mu_{\text{thresh}}$  and  $\sigma_{\text{thresh}}$  by using statistics method. 12 000 halftone images are used as the experiment subjects and each image is divided into many sub-image blocks with  $K \times K$  size.  $\mu$  and  $\sigma$  of sub-image blocks are acquired via (7) and (8) respectively to construct two histograms as shown in Fig. 3. The amount of sub-image blocks involved in statistics will decrease with increasing  $K$ . If  $K=32$  (256), the amount of sub-image blocks reaches to 768 000 (12 000). Fig. 3(a) shows the histograms of  $\mu$  obeying Gaussian distribution approximately. Fig. 3(b) indicates histograms of  $\sigma$  also obeying Gaussian distribution approximately. Now we get  $\mu_{\text{thresh}}$  by forcing  $\mu$  of 95% sub-image blocks to satisfy  $\mu > \mu_{\text{thresh}}$  and get  $\sigma_{\text{thresh}}$  by forcing  $\sigma$  of 95% sub-image blocks to satisfy  $\sigma < \sigma_{\text{thresh}}$ . TABLE III shows  $\mu_{\text{thresh}}$ ,  $\sigma_{\text{thresh}}$  and proportion of invalid images with different  $K$ . From TABLE III, we can conclude that the proportion of invalid images will increase with the increase of  $K$ , so in practice,  $K$  can't be set too large. Generally  $K=32 \sim 128$ .

#### B. Experiment 2

We extract the features from 40 halftone images of each type of halftone patterns via MDC ( $K=128$  and  $L=8$ ) to plot the curves shown in Fig. 4 in this experiment. Fig. 5 shows the feature curves obtained by EODC. From Fig. 4 and Fig. 5, we can conclude that the difference of feature curves among sub-figures in Fig. 4 is more distinct than that in Fig. 5. Furthermore, feature curves in Fig. 4 are more consistent than that in Fig. 5. On the other hand, the computation cost of MDC is lower than that of EODC resulting in less time expense. In our experiments, the

time costs of MDC and EODC are 32 ms and 56 ms respectively.

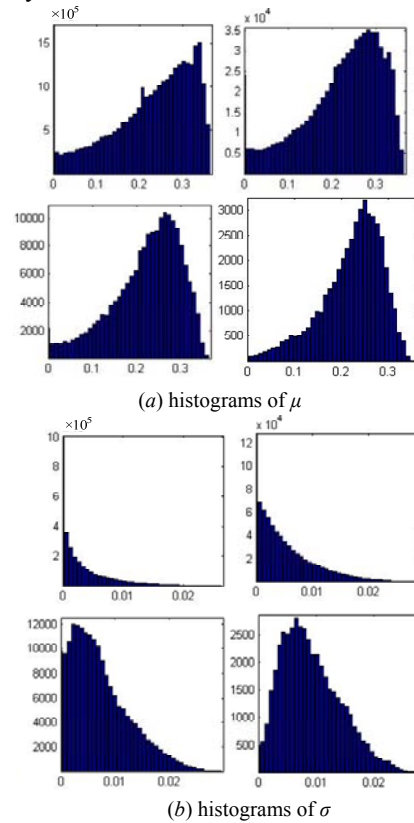


Figure 3. Histograms.  $K=32, 64, 128, 256$  respectively.

TABLE III.  
THRESHOLD AND PROPORTION OF INVALID IMAGE

$K$	Proportion of invalid image (%)	$\mu_{\text{thresh}}$	$\sigma_{\text{thresh}}$
32	0.015	0.009	0.013
64	0.14	0.037	0.016
128	1.01	0.075	0.018
256	6.48	0.101	0.019

#### C. Experiment 3

To evaluate the performance of the presented method, we use the neural network as classifier and regard the classification correct rate as performance evaluation of feature extraction algorithm. BP neural networks and Radial Basis Function (RBF) neural networks are two most popular methods of all neural networks, but slow training speed of BP neural network is obstacle for application. Therefore, we use RBF neural network as classifier. The structure of RBF network is shown in Fig. 6. In Fig. 6, The output vector of network  $Y=\{y_1, y_2, \dots, y_{12}\}$ , Input vector  $X=\{x_1, \dots, x_n\}$  and  $q=\{q_1, \dots, q_n\}$ .  $n=3L$  in MDC but  $n=16$  in EODC. Function  $\varphi$  is a radial basis Gaussian function.  $y_i$  of  $Y$  describes the category of a halftone image, for example,  $y_i=1$  and  $y_j=0$  ( $\forall j|1 \leq j \leq 12$  and  $j \neq i$ ) mean  $i$ th class ( $1 \leq i \leq 12$ ). We can decide the category of input vector  $X$  by  $c = \arg \max_i \{y_i\}$ .

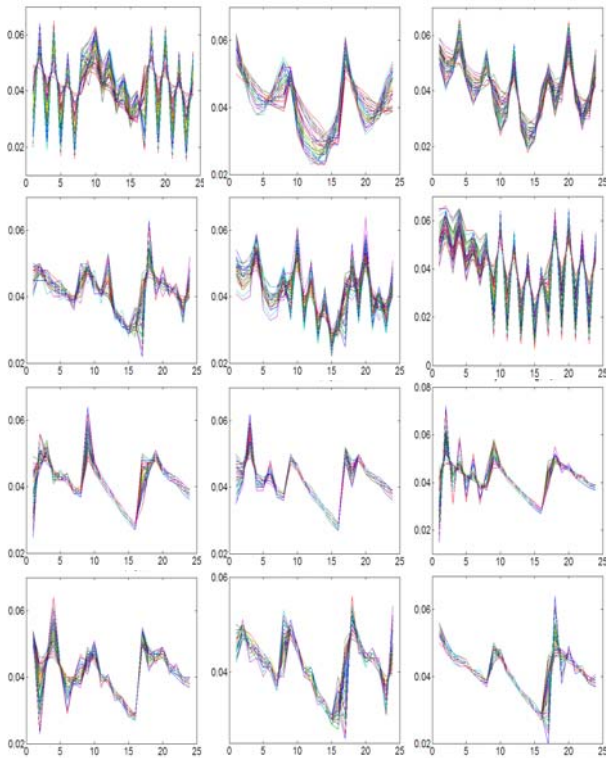


Figure 4. Feature curve extracted by MDC ( $K=128$  and  $L=8$ ), where the X-axis denotes the feature number and Y-axis denotes the feature value.

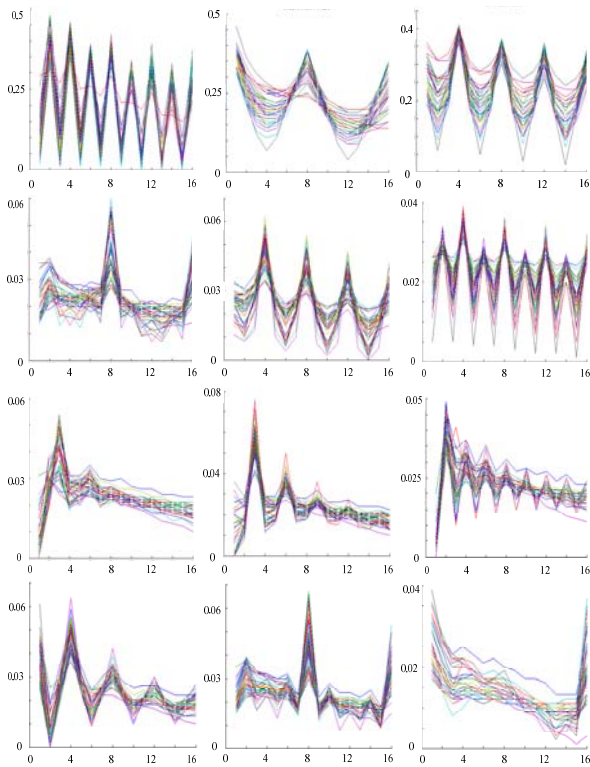


Figure 5. Feature curve extracted by EODC ( $L=16$ ), where the X-axis denotes the feature number and Y-axis denotes the feature value.

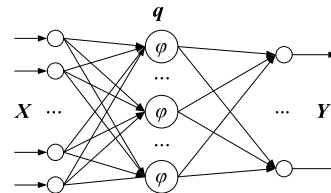


Figure 6. RBF network structure

In multi-class problem, there are two parameters: average classification correct rate (ACCR) and classification correct rate variance (CCRV). Next, we will compare the performance of the proposed method (MDC+RBF) against two similar methods. The first similar method is the BP based on EODC (EODC+BP) in which EODC ( $L=16$ ) is employed to extract features of halftone images and BP neural network is used to classify these images. The second is the method based on least mean square (LMS) and Bayes method (LMS+Bayes) [8] in which Fourier spectrums of halftone images are utilized as input of LMS. TABLE IV gives ACCR and CCRV of above three methods from which we know the ACCR of MDC+RBF ( $K=128, L=8$ ) is highest, namely 98.42% and CCRV of MDC+RBF is lowest.

To further test our method, another comparison is conducted in this experiment. MDC (two case:  $K=64$  and  $L=8, K=128$  and  $L=8$ ) is used to extract the features of halftone images and performance of five classifications is compared. Five classifications are RBF neural network (RBF), support vector machine (SVM) [13], BP neural network (BP) [14], principal component analysis [15] for feature dimension reduction and nearest neighbor algorithm (PCA+NN), and only nearest neighbor algorithm (NN). ACCR and CCRV of above five methods are shown in TABLE V from which we conclude that RBF is best for classification of features obtained by MDC.

TABLE IV. PERFORMANCE OF CLASSIFICATION

performance	MDC+RBF	EODC+BP	LMS+Bayes
ACCR(%)	98.42	94.05	96.39
CCRV(%)	0.96	2.57	3.53

TABLE V. PERFORMANCE OF CLASSIFICATION

Param	evaluation	RBF	BP	SVM	PCA+NN	NN
$K=64, L=8$	ACCR(%)	98.11	93.6	90.51	94.95	95.2
	CCRV(%)	1.02	2.81	8.53	6.79	6.34
$K=128, L=8$	ACCR(%)	98.42	94.1	89.59	96.24	96.9
	CCRV(%)	0.96	2.34	9.39	4.53	4.1

In order to observe the presented method more clearly, we will discuss how to select parameters ( $K$  and  $L$ ). Let both  $L$  and  $K$  are the power of 2 satisfying  $L \leq K$  in our experiments. ACCR of different  $L$  value and different  $K$  value are shown in Fig.7. From Fig.7, we know that for specified  $L$ , ACCR will reach to maximum, namely 98.42% if  $K=128$ . On the other hand, for specified  $K$ , ACCR will reach to maximum if  $L=8$ . So we can

conclude if  $K=128$  and  $L=8$ , ACCR is the best, namely the feature extraction method is best.

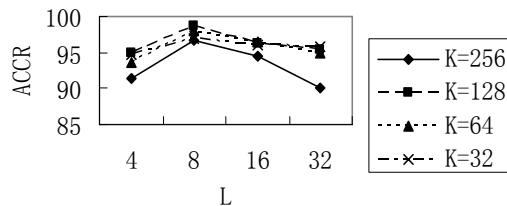


Figure 7. Classification performance of different  $K$  and  $L$

#### IV. CONCLUSION

Classification of halftone image is one of the crucial methods to resolve the optimal reconstruction problem of halftone images. The research of this paper focuses on feature extraction of halftone images. A new multi-directional correlation feature of halftone images is presented and a decision rule is introduced to reject invalid halftone image. Furthermore, a feature extraction algorithm of halftone image based on effective sub-image block is proposed. The experiment results show the proposed method is better than other similar methods. At present, since there are little research for halftone image classification, further studies should be needed to meet digital society. More effective learning and classification method are in urgent need. All these are our future work.

#### ACKNOWLEDGEMENTS

This work was supported by National Natural Science Foundation in China under Grant No. 61170102, Natural Science Fund of Hunan province in China under Grant No.11JJ3070, and Education Department Fund of Hunan province in China under Grant No. 12A039.

#### REFERENCES

- [1] P. Freitas, M. Farias, A. Araujo, "Fast Inverse Halftoning Algorithm for Ordered Dithered Images," in *Graphics, Patterns and Images, 24th SIBGRAPI Conference on*, April, pp.250-257, 2011.
- [2] Saika Y, Okamoto K, Matsubara F. "Probabilistic Modeling to Inverse Halftoning based on Super Resolution," in *Control, Automation and Systems, 2010 International Conference on*, October, pp.162-167, 2010.
- [3] R. Stevenson, "Inverse Halftoning via MAP Estimation," *Image Processing, IEEE Trans. on*, vol.6, no.4, pp.574-583, 1997.
- [4] G. B. Unal, A. E. Cetin, "Restoration of error-diffused images using projection onto convex sets," in *Images Processing, IEEE Trans. on*, vol.10, no.12, pp.1836-1841, 2001.
- [5] M. Mese, P. Vaidyanathan, "Optimized halftoning using dot diffusion and methods for inverse halftoning," *Images Processing, IEEE Trans. on*, vol.9, no.4, pp.691-709, 2000.
- [6] P. C. Chang, C. S. Yu, "Neural net classification and LMS reconstruction to halftone images," in *Proc. of SPIE-The International Society for Optical Engineering*, vol. 3309, pp. 592-602, 1997.
- [7] Y. P. Kong, P. Zeng, Y. P. Zhang, "A Classification and Recognition Algorithm for Halftone Image," in *Journal of Xidian University*, vol.38, no.5, pp.62-69, 2011.
- [8] Y. F. Liu, J. M. Guo, J. D. Lee, "Halftone Image Classification Using LMS Algorithm and Naive Bayes," in *Image Processing, IEEE Trans. on*, vol.20, no.10, pp.2837-2847, 2011.
- [9] R. Ulichney, "Digital halftoning and the physical reconstruction function," *Ph.D. Thesis*, Dept. of Electrical Engineering and Computer Science, Massachusetts Institute of Technology, Massachusetts, United States, 1986.
- [10] D. E. Knuth, "Digital halftones by dot diffusion," in *ACM Trans. Graph.*, vol. 6, no. 4, pp. 245-273, 1987.
- [11] R. Ulichney, "Dithering with blue noise," in *Proc. of the IEEE*, Vol.76, no.1, pp. 56-79, 1988.
- [12] M. Mese, P. P. Vaidyanathan, "Optimized halftoning using dot diffusion and methods for inverse halftoning," in *Image Processing, IEEE Trans. on*, Vol.9, no.4, pp.691-709, 2000.
- [13] Y. Wei, X. Wu, "A New Fuzzy SVM based on the Posterior Probability Weighting Membership," in *Journal of Computers*, vol.7, no.6, pp.1385-1392, 2012.
- [14] Q. Chen, K. Huang, X. Yang, et al, "A BP Neural Network Realization in the Measurement of Material Permittivity," In *Journal of Software*, vol.6, no.6, pp.1089-1095, 2011.
- [15] Q. Zhao, "The Study on Rotating Machinery Early Fault Diagnosis based on Principal Component Analysis and Fuzzy C-means Algorithm," in *Journal of Software*, vol 8, no 3, pp.709-715, 2013.



**Zhiqiang Wen** was born in China in 1973. He received the MS degrees in technology of computer application from Guangxi University, China, in 2004 and PhD degree in technology of computer application from the Central South University, China, in 2008. Since 2009, He has been an associate professor of School of Computer and Communication, Hunan University of Technology, Hunan zhuzhou, China and is the member of China computer Federation. His research interests include computer vision, digital image processing and robotics.



**Yongxiang Hu** was born in China in 1973. He received the MS degrees in technology of computer application from Hua Nan normal University, China, in 2005 and PhD degree in biomedical engineering from the Central South University, China, in 2012. Since 2008, He has been an associate professor of School of Computer and Communication, Hunan University of Technology, Hunan zhuzhou, China. His research interests include image processing and pattern recognition.



**Wenqiu Zhu** was born in China in 1968. He received the MS degrees in Software Engineering from the Central South University, China, in 2005. Since 2008, He has been a professor of School of Computer and Communication, Hunan University of Technology, Hunan zhuzhou, China. His research interests include digital image processing and

pattern recognition.